

Nanoparticle-enhanced thin film solar cells: Metallic or dielectric nanoparticles?

Yu. A. Akimov,^{1,a)} W. S. Koh,¹ S. Y. Sian,² and S. Ren²

¹*Advanced Photonics and Plasmonics Team, Institute of High Performance Computing, 1 Fusionopolis Way, #16-16 Connexis, Singapore 138632*

²*National University of Singapore, 9 Engineering Drive 1, Singapore 117576*

(Received 11 January 2010; accepted 21 January 2010; published online 18 February 2010)

Recently, thin film solar cells enhanced by nanoparticles have attracted much attention of the scientific community. To improve the performance of such cells, a systematic study on the influence of the nanoparticle material on the efficiency of the enhancement is performed. Based on optimization of the nanoparticle array parameters, the role of dispersion and dissipation of the nanoparticle material is discussed and analyzed with respect to optical absorption of the photoactive layer. Finally, it is demonstrated that the use of dielectric nanoparticles can lead to similar and even higher enhancements compared to that of metal nanoparticles. © 2010 American Institute of Physics. [doi:10.1063/1.3315942]

In order for solar cells to compete with other forms of commercially produced energy, their manufacturing costs must be reduced. To address this need, thin film solar cells were proposed as a low cost alternative to conventional wafer-based solar cells.¹ Apart from being fabricated by a process that utilizes less energy and causes less wastage, thin film solar cells are only a few micrometers thick and hence, require less semiconductor material to manufacture than wafer-based cells. However, this compromises their performance due to poor light absorption and requires more efficient light-trapping techniques as compared to traditional texturing schemes that may not be suitable for micron and submicron cells.^{1,2}

Recent research into the field of plasmonics has found an alternative way to improve light-trapping of thin film solar cells by using plasmon-enhanced light scattering from metal nanoparticles deposited on the cell surface.³ Through interaction with surface plasmons of the metal nanoparticles, the incident light is resonantly scattered and coupled at high scattering angles with the trapped waveguide modes of the photoactive layer.²⁻⁴ This significantly increases the optical path of light in the active layer and improves photoelectron generation.

Despite initial studies focused mainly on thin film solar cells enhanced with nanoparticles of noble metals,²⁻⁹ there is still no systematic study on the influence of the nanoparticle material on such enhancements. Moreover, improved light-trapping of thin films due to scattering from small particles is not limited to metal nanoparticles. In fact, similar enhancement can also be realized with dielectric nanoparticles.^{10,11}

It is clear that the optical properties of metals and dielectrics are different, and that the degree of enhancement associated with each group of materials is different as well. Through coupling with surface plasmons, metallic nanoparticles can provide very efficient scattering of light. However, they also exhibit extraordinary absorption at the surface plasmon resonances.¹² This significantly decreases the overall effect of metallic nanoparticles.^{8,9} On the other hand, dielectric nanoparticles can also provide sufficient scattering, espe-

cially if their dielectric permittivity is quite high.¹² Moreover, a number of dielectrics possess a very low dissipation level at visible wavelengths. Based on this argument, it is expected that dielectric nanoparticles can exhibit comparable or even better enhancement in solar cell performance. In addition, such nanostructures can be synthesized using a variety of conventional deposition techniques similar to the ones used for solar cell manufacturing.^{13,14}

To study and compare the performance of nanoparticle-enhanced solar cells using metallic and dielectric nanoparticles, we consider a three-dimensional model of an amorphous silicon solar cell of the type ITO(20 nm)/*a*-Si:H(240 nm)/Al(80 nm). The deposited nanoparticles are assumed to be spherical and distributed in a square arrangement on top of the ITO layer. Simulations were run on COMSOL Multiphysics, where Maxwell's equations were solved for monochromatic, perpendicularly incident plane waves. Periodic and perfectly matched layer boundary conditions were applied to the model to account for multiple scattering and cross-coupling of neighboring nanoparticles in the array. Enhancement in solar cell photoelectron generation was then computed by integration of the power absorbed in the *a*-Si:H layer over the AM1.5G spectrum and subsequent normalization by the value calculated for the reference cell without any nanoparticles.

The efficiency of light scattering into the amorphous silicon active layer, and hence, photocurrent enhancement, depends on the nanoparticle radius R , percentage surface coverage η , and material permittivity ϵ . It is expected that for each material, there exist certain combinations of the radius and surface coverage that maximize the photocurrent enhancement.⁹ To find these combinations, we have optimized the radius and the surface coverage of nanoparticles for maximum power absorption by the *a*-Si:H layer. We have restricted the radius values to the range from 0 to 50 nm, and the surface coverage to the range from 0% to 78.5%.

It is clear that the total power absorbed in the photoactive region is determined by the nanoparticle permittivity $\epsilon(\omega)$ and its frequency dependence. To consider its effect, we expand $\epsilon(\omega)$ near $\omega_0=2$ eV, where the reference cell

^{a)}Electronic mail: akimov@ihpc.a-star.edu.sg.

exhibits maximum in the spectrum for the optically absorbed power,⁹

$$\varepsilon(\omega) = \text{Re}[\varepsilon(\omega_0)] + \frac{\partial \text{Re}[\varepsilon(\omega)]}{\partial \omega} \bigg|_{\omega_0} (\omega - \omega_0) + O[(\omega - \omega_0)^2] + i \text{Im}[\varepsilon(\omega)]. \quad (1)$$

Here, the first term is considered as nondispersive, while the others are frequency-dependent and account for dispersion (the second and third terms) and energy dissipation (the fourth term) of the nanoparticle material.

Note that for real materials, dispersion and dissipation effects cannot be studied independently, since they together describe such unique features as resonant scattering and absorption by nanoparticles.¹² For example, scattering and absorption cross-sections of an extremely small (compared to the wavelength of the incident light, λ) spherical particle can be written as

$$\sigma_{\text{sca}} = \frac{1}{6\pi} \left(\frac{2\pi}{\lambda} \right)^4 |\alpha|^2, \quad \sigma_{\text{abs}} = \frac{2\pi}{\lambda} \text{Im}(\alpha), \quad (2)$$

where

$$\alpha = 4\pi R^3 \frac{(\varepsilon - 1)}{(\varepsilon + 2)} \quad (3)$$

is the polarizability of the particle. Cross-sections (2) exhibit the surface plasmon resonance, when ε is close to -2 and the polarizability α becomes very high. This resonance can be excited in metallic particles owing to dispersion of metals [$\partial \text{Re}(\varepsilon)/\partial \omega \neq 0$] that makes it possible for $\text{Re}(\varepsilon)$ to reach negative values. At the same time, the dissipation term $\text{Im}(\varepsilon)$ in Eq. (1) determines the resonant values of both σ_{sca} and σ_{abs} .¹² Thus, dispersion and dissipation effects of the nanoparticle material should be studied simultaneously.

The overall influence of dispersion and dissipation of the nanoparticle material can be analyzed by comparing the enhancements caused by nanoparticles of existing materials with complex permittivity $\varepsilon(\omega)$ and those of ideal materials, characterized by constant permittivity $\varepsilon_0 = \text{Re}[\varepsilon(\omega_0)]$ and zero dissipation. For ideal nanoparticles, we performed simulations for different non-dispersive and nonabsorbing materials with $\varepsilon(\omega) = \varepsilon_0$ in a very broad range of real constants ε_0 . The maximum enhancement of the absorbed power in the photoactive layer obtained after optimization of the size and coverage of such nanoparticles is shown in Fig. 1. It reveals that the enhancements by ideal nanoparticles grow with the absolute value of the permittivity and saturate for highly negative and positive ε_0 at around 32%. This is consistent with the polarizability of a single particle (3) that tends to the same limit, $\alpha = 4\pi R^3$, for extremely high positive and negative values of ε .

It is interesting that for permittivities in the range $(-2; 1)$ the ideal particle polarizability α changes its sign and becomes negative. Such nanoparticles deposited onto a cell reflect more light back, decreasing the overall absorption by the cell. This results in “negative enhancements” by ideal nanoparticles and zero maximum enhancement that corresponds to the reference cell case, when $\eta = 0$. Furthermore, outside of the range $(-2; 1)$, α grows with dielectric permittivity, so that negative values of ε always give higher polarizability than positive ε . This explains why the optimum values of R and η for ideal metals (negative permittivity) and

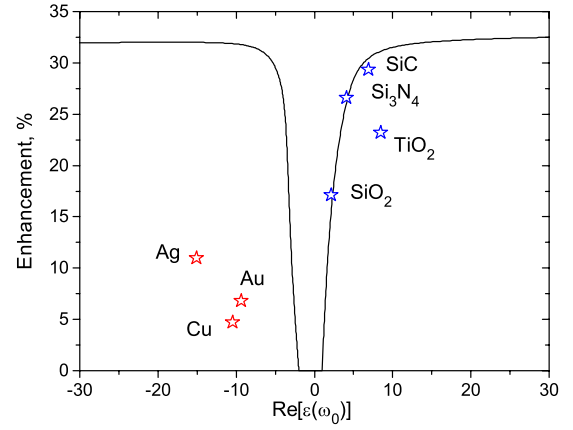


FIG. 1. (Color online) Maximum enhancement that can be reached by nanoparticles of different materials characterized with $\text{Re}(\varepsilon)$ at $\omega_0 = 2$ eV. Optimum enhancements for ideal nanoparticles with $\text{Re}[\varepsilon(\omega_0)] = \varepsilon_0$ are shown by the solid line. Stars depict the maximum enhancement by real metals and dielectrics.

ideal dielectrics (positive permittivity) exhibit very different behavior, as depicted in Fig. 2. For $\varepsilon_0 \in (-\infty; -2)$, particle polarizability α increases from $4\pi R^3$ to infinity, while for $\varepsilon_0 \in [1; \infty)$ it changes from zero to $4\pi R^3$. Smaller polarizabilities of particles require higher surface coverage and larger size of the particles in order to reach the same scattering level. This results in more dense optimum packaging for the particles of ideal dielectrics with $\varepsilon_0 > 1$. Moreover, for permittivities close to unity, the optimum configuration of nanoparticles requires extremely dense packaging with $\eta = \pi/4$ [Fig. 2(b)].

So far, we have discussed the effects of the ideal nanoparticles, revealing the contribution of the nondispersive term $\text{Re}[\varepsilon(\omega_0)] = \varepsilon_0$ of Eq. (1) to the nanoparticle enhancement. This contribution can result in an enhancement of up to 32%. However, nonzero dispersion and absorption terms of real materials can significantly change this value. For example, the maximum enhancements provided by the commonly used metals (Ag, Au, and Cu) are much lower (by over 20%) than that of the ideal metals (Fig. 1). This is attributed to the high attenuation of metallic nanoparticles caused by excitation of surface plasmons in the visible range,

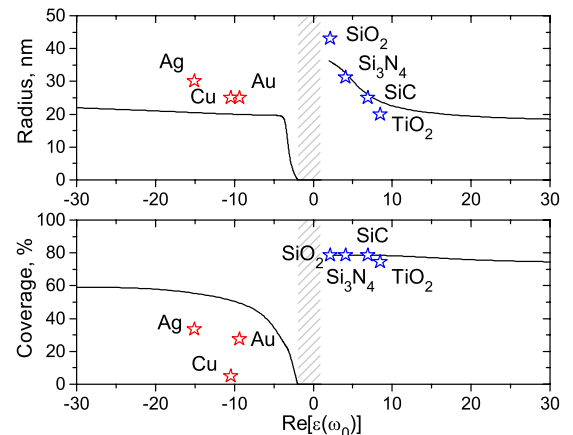


FIG. 2. (Color online) Optimum (a) radius and (b) surface coverage of the nanoparticles maximizing the enhancement, as functions of $\text{Re}[\varepsilon(\omega_0)]$. The optimum characteristics of ideal nanoparticles are shown by the solid lines. The shaded region shows the range where the ideal nanoparticles result in nonpositive effects.

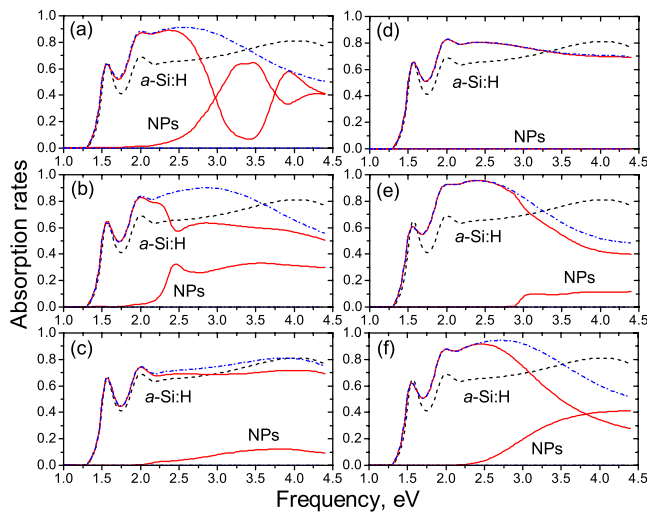


FIG. 3. (Color online) Spectral absorption rates of the *a*-Si:H layer and the nanoparticle array (the solid lines) optimized for (a) Ag, (b) Au, (c) Cu, (d) SiO₂, (e) SiC, and (f) TiO₂ nanoparticles. The reference cell response is plotted as the dashed line; the dash-dotted lines show the contribution of the nondispersive term $\text{Re}[\epsilon(\omega_0)]$.

as shown in Figs. 3(a)–3(c). Even for the optimized parameters, metallic nanoparticles absorb up to 60% of the sunlight energy in the resonant region, as in the case of Ag nanoparticles. This leads to a dramatic decrease in the enhancement compared to the contribution by the nondispersive term $\text{Re}[\epsilon(\omega_0)]$, especially at frequencies above 2.25 eV. At the same time, at frequencies below the surface plasmon resonance, the absorption of metal nanoparticles goes down, resulting in enhancements approaching those by ideal particles. Nevertheless, the high resonant absorption of metal nanoparticles makes the overall cumulative effect of dispersion and dissipation negative and results in quite strong heating of the nanoparticles.

Thus, to reach higher enhancement efficiencies, low-dissipative, and low-dispersive materials should be used instead of highly absorbing metals. In addition, the absolute value of the dielectric permittivity $\text{Re}[\epsilon(\omega_0)]$ should be as high as possible (Fig. 1). These conditions can easily be fulfilled for dielectric nanoparticles. Figures 3(d)–3(f) show the spectral absorption of the cells enhanced with different dielectric particles. These figures reveal that small dispersion of the dielectrics leads to negligible changes, while the finite dissipation, such as in the cases of SiC and TiO₂, leads to

negative deviation from the case of ideal dielectrics. Furthermore, the obtained results suggest that even low-permittivity dielectrics, such as silicon dioxide with $\text{Re}[\epsilon(\omega_0)]=2.12$, can provide higher overall enhancements compared to plasmonic metals (Fig. 1). However, the choice of dielectric is always a compromise between high dielectric permittivity and low dissipation level, as shown in Figs. 3(d)–3(f).

In conclusion, we have performed optimization of the nanoparticle parameters, such as size, surface coverage, and material of the particles, and demonstrated that dielectric particles can result in similar and even several times higher enhancements compared to the commonly used plasmonic metals. We have shown that some dielectrics with quite high permittivity, such as silicon carbide with $\text{Re}[\epsilon(\omega_0)]=6.96$, can reach almost 30% enhancement (close to the ideal limit of 32%). Additionally, they feature very high surface density, which can easily be obtained under self-assembly of the nanoparticles.^{10,11} Thus, we have proven, with the aid of numerical modeling, that the deposition of dielectric particles with high permittivity and low dissipation level can significantly enhance photoelectron generation and hence, result in better performance of thin film solar cells.

The authors would like to acknowledge Professor W. J. R. Hoefer for his valuable comments on the manuscript.

¹M. A. Green, *Solar Cells: Operating Principles, Technology and System Applications* (The University of New South Wales, Sydney, 1998).

²K. P. Catchpole and A. Polman, *Appl. Phys. Lett.* **93**, 191113 (2008).

³K. R. Catchpole and A. Polman, *Opt. Express* **16**, 21793 (2008).

⁴H. R. Stuart and D. G. Hall, *Appl. Phys. Lett.* **73**, 3815 (1998).

⁵D. M. Schaadt, B. Feng, and E. T. Yu, *Appl. Phys. Lett.* **86**, 063106 (2005).

⁶D. Derkacs, S. H. Lim, P. Matheu, W. Mar, and E. T. Yu, *Appl. Phys. Lett.* **89**, 093103 (2006).

⁷Yu. A. Akimov, K. Ostrikov, and E. P. Li, *Plasmonics* **4**, 107 (2009).

⁸K. Nakayama, K. Tanabe, and H. A. Atwater, *Appl. Phys. Lett.* **93**, 121904 (2008).

⁹Yu. A. Akimov, W. S. Koh, and K. Ostrikov, *Opt. Express* **17**, 10195 (2009).

¹⁰T. H. Chang, P. H. Wu, S. H. Chen, C. H. Chan, C. C. Lee, C. C. Chen, and Y. K. Su, *Opt. Express* **17**, 6519 (2009).

¹¹C.-P. Chen, P.-H. Lin, L.-Y. Chen, M.-Y. Ke, Y.-W. Cheng, and J. J. Huang, *Nanotechnology* **20**, 245204 (2009).

¹²C. F. Bohren and D. R. Huffman, *Absorption and Scattering of Light by Small Particles* (Wiley, New York, 1998).

¹³Q. J. Cheng, S. Xu, J. D. Long, and K. Ostrikov, *Appl. Phys. Lett.* **90**, 173112 (2007).

¹⁴S. Xu, I. Levchenko, S. Y. Huang, and K. Ostrikov, *Appl. Phys. Lett.* **95**, 111505 (2009).